IJICIS, Vol.21, No.1, 149-164
DOI: 10.21608/ijicis.2021.66637.1068

International Journal of Intelligent Computing and Information Sciences

https://ijicis.journals.ekb.eg/

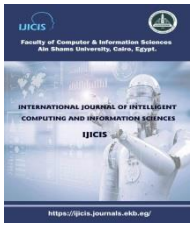

REPURPOSING ANTIVIRAL DRUGS TO INHIBIT SARS-COV-2 PAPIN-LIKE PROTEASE ACTIVITY

Ibrahim Khater

Biophysics Department,
Faculty of Science, Cairo University,
Giza, Egypt
ikhater@sci.cu.edu.eg

Aaya Nassar*

Biophysics Department,
Faculty of Science, Cairo University,
Giza, Egypt
aaya_nassar@cu.edu.eg

Received 2021- 3-7; Revised 2021-5-20; Accepted 2021-5-28

Abstract: *Since December 2019, a pneumonia caused by a novel coronavirus (SARS-CoV-2) emerged in China and has rapidly spread around the world. The virus has caused a global outbreak of viral pneumonia, which has been known as coronavirus disease (COVID-19). This study aims to examine known direct acting antivirals (DAA) against SARS-CoV-2 papin like protease. A number of known antiviral drugs were tested as potential SARS-CoV-2 virus inhibitors using the molecular docking analysis to examine the free natural affinity of the binding ligand to catalytic residues and substrate binding pockets without forcing the docking of ligand to active site. SARS-CoV-2 papin like protease solved structure (PDB ID: 6W9C) is targeted by direct acting antiviral drugs. The geometry of all inhibitors was optimized using Avogadro software. Molecular Docking was performed using AutoDock Vina software. Protein-Ligand Interaction Profiler (PLIP) web server was used to analyze the interactions formed between drugs and SARS-CoV-2 PLpro. Mycophenolic acid and 4'-Tosyl Mycophenolic Acid-d3 was tested against SARS-CoV-2 papin like protease mutant C111S (PDB ID: 6WRH). Mycophenolic acid showed mild efficacy against the mutant strain. The molecular docking analysis results indicated that Mycophenolic acid and 4'-Tosyl Mycophenolic Acid-d3 has good binding affinities to the protein drug target (-5.72 Kcal/mol and -5.72 Kcal/mol) and showed the highest probabilities to bind to catalytic residues of target protein (30% and*

* Corresponding author: Aaya Nassar
Biophysics Department, Faculty of Science, Cairo University, Giza, Egypt
E-mail address: aaya_nassar@cu.edu.eg

50%) respectively, suggesting their potential use for COVID-19 treatment. Molecular dynamic simulation was used to confirm the stability of the complexes formed.

Keywords: *Coronavirus treatment, 4'-Tosyl Mycophenolic Acid-d3, molecular docking, anti-protease drugs*

1. Introduction

In late December 2019, a new type of coronavirus originated in Wuhan, China, began to spread across the world. The virus caused a global health outbreak of viral pneumonia, which has been named coronavirus disease (COVID-19) caused by the severe acute respiratory syndrome coronavirus 2 (SARS-CoV-2). As of February 14, 2021, total of 108,818,442 cases and 2,396,175 deaths had been confirmed worldwide including 213 countries, areas, or territories (1). On 30 January 2020, the World Health Organization (WHO) declared the outbreak as a Public Health Emergency of International Concern (PHEIC) (2) and on 11 March 2020, WHO declared it as a global pandemic (3). Since then, many scientific journals published a number of articles, comments, editorials and perspectives related to COVID-19, trying to understand the virus structure, behavior and features to find possible treatments to the newly emerged COVID-19 disease (4).

Various viral epidemics related to coronavirus were reported over the past 20 years including the severe acute respiratory syndrome coronavirus (SARS-CoV) emerged in 2002 and the swine flu H1N1 virus in 2009 while the Middle East respiratory syndrome coronavirus (MERS-CoV) was first identified in Saudi Arabia in 2012 (4). Human respiratory viruses like coronavirus (HCoVs) are one of the major pathogens that infect the human upper respiratory tract. Previous outbreaks of coronaviruses include 229E and NL63 strains which belong to *Alphacoronaviruses*, while OC43, HKU1, SARS, and MERS belong to *Betacoronaviruses* (5). SARS and MERS are the most aggressive strains of coronaviruses along with the newly developed human coronavirus SARS-CoV-2 that was first reported in December 2019 in China (5), (6). The SARS-CoV-2 virus is contagious and widely spreading worldwide. The genomic sequence analysis of SARS-CoV-2 showed 88% identity with SARS (7), (8). SARS-CoV-2 is a member of *Betacoronaviruses* like SARS and MERS (9). The comparative analysis of the diseases etiology showed similarities in the symptoms between SARS-CoV-2 and other *Betacoronaviruses* (10). Symptoms of COVID-19 infection appear to start approximately 5 days after contracting the virus, and the period from COVID-19 symptoms to reported death cases ranged from 6 to 41 days with a median of 14 days depending on the age of the patient and the status of the patient's immune system and other underlying health conditions comorbidities. The common symptoms of COVID-19 are chills, fever of 100.4 F, dry cough, fatigue, headache, hemoptysis, diarrhea, dyspnea, nausea, olfactory loss of taste or smell and lymphopenia (8), (10), (11), (12), (13). Commonly, HCoVs are positive-sense and are very long single-stranded RNA viruses (30,000 bp). HCoVs consists of two groups of proteins; four structural proteins, such as Spike (S) that characterize all coronaviruses, Nucleocapsid (N), Matrix (M), and Envelope (E), in

addition to non-structural proteins such as proteases (nsp3 and nsp5) and RNA-dependent-RNA polymerase RdRp (nsp12) and main protease (Mpro) and papain-like protease (PLpro) (14).

The papain-like protease domain (PLpro) and the main protease (Mpro) are together responsible for processing the viral polyproteins yielding mature viral proteins (15), (16), (17). The PLpro of SARS-CoV-2 plays crucial role in virus replication and immune evasion, making PLpro enzyme a potential drug target (18), (19). Taking into consideration the shared homology between PLpro proteases of SARS-CoV-2 and SARS-CoV, where SARS-CoV2-PLpro and SASR-CoV-PLpro share 83% sequence identity, makes inhibitors developed for SARS-CoV PLpro a significant insight for developing therapeutics for SARS-CoV-2 and makes PLpro a significant antiviral drug target (20), (21).

Coronaviruses such as the SARS virus and the MERS virus encode at least one papain-like protease (PLpro) enzyme in their genomes, which cleaves the viral replicase polyproteins at three sites releasing non-structural protein nsp1, nsp2 and nsp3. The SARS-CoV nsp3 multi-domain protein is the largest replicase subunit at 1,922 amino acids (22), (23). Nsp3 plays a vital role in the formation of virus replication complexes by its insertion into the host membrane and interacting with other nsps (24) especially nsp4 and nsp6 (25). SARS-CoV PLpro cleaves ubiquitin and ISG15, known regulators of host innate immune pathways, and inhibition of SARS-CoV PLpro has been shown to block SARS-CoV replication (26). PLpro possesses deubiquitinating and deISGylating activities, which have been proposed to suppress the host antiviral response by counteracting the post-translational modification of signaling molecules that activate the innate immune response, PLpro is made up of an N-terminal ubiquitin-like domain found in many ubiquitin-specific proteases (USPs) (27) and a C-terminal catalytic domain containing a right-handed fingers, palm, and thumb domain organization (28). Maiti et al. showed that sulfur-based drugs and peptides-based inhibitors may block Cys residues in the catalytic site and/or Zn site of SARS-CoV-2-PLpro, leading to dysfunction of SARS-CoV-2-PLpro and thereby halting the viral replication (29). On the other hand, Alamri et al. detected three compounds ADM_13083841, LMG_15521745, and SYN_15517940 that showed stable conformation and interacted well with the active residues of SARS-CoV-2 PLpro (30), whereas Alfaro et al. indicated that Schizanthine Z binds to the SARS-CoV-2 papain-like protease with relatively high affinity (31). In addition, Li et al. found that Neobavaisoflavone has high binding energy for SARS-CoV-2 papain-like protease and could bind near the SARS-CoV-2 papain-like protease catalytic triad (32). Kouznetsova et al. showed sixteen FDA approved drugs, including chloroquine and formoterol to bind to PLpro with significant affinity and good geometry, suggesting their potential use against the virus (33).

In this research study, molecular docking was applied to examine the binding affinity of different direct acting antivirals (DAAs) against the SARS-CoV-2 papin-like protease (PLpro). The crystal structure of papain-like protease of SARS-CoV-2 (PDB ID: 6W9C) was downloaded from the protein data bank (PDB) database and prepared for the docking experiment using AutoDock automated tools. DAAs were downloaded from the drug databank, DrugBank, (www.drugbank.ca) (34) and optimized using MMFF94 force field function of Avogadro software (https://avogadro.cc) (35). AutoDock Vina software

(http://vina.scripps.edu) (36) was used in this study to dock the optimized DAAs against SARS-CoV-2 PLpro. The results from docking, the docking complexes, were then analyzed using the Protein-Ligand Interaction Profiler (PLIP) web server of Technical University in Dresden (37). GROMACS software (38) was used to provide the information about the stability of the molecular interactions on the docking complexes. PLpro was introduced to 1000 ps molecular dynamics simulation (MD) and compressed coordinates were retrieved every 10 ps (100 frames). Molecular docking was performed between DAAs of highest probability to bind to catalytic residues and different frames of PLpro MD. Molecular docking was then applied to test the binding affinity of different DAAs against SARS-CoV-2 papin-like protease mutant C111S stain.

The main purpose of this study is to test potential inhibitors against SARS-CoV-2 using molecular docking analysis. The study investigates a number of recently researched drugs for their binding interactions then to evaluate their potential use for COVID-19 treatment.

2. Materials and Methods

2.1. SARS-CoV-2 PLpro Structure

The complete genome sequence of the newly emerged SARS-CoV-2 (NC_045512.2) is retrieved from the National Center for Biotechnology Information (NCBI) nucleotide database (GenBank: NC_045512.2, https://www.ncbi.nlm.nih.gov/nuccore/NC_045512). SARS-CoV-2 PLpro solved structure was retrieved from Protein Data Bank (PDB ID: 6W9C, available at https://www.rcsb.org/structure/6W9C). The catalytic residues of SARS-CoV PLpro are within hydrogen-bonding distance of one another, suggesting the existence of protonation state of Cys112 in equilibrium with His273 and Asp287 (21). However, due to missing of some residues in crystallographic structure of PLpro (PDB ID: 6W9C) the order of the catalytic residues turns out to be (Cys111, His272 and Asp286).

The inhibitor for SARS-CoV PLpro is the binding site for docking. The binding site has more S3/S4 pockets than the restrictive substrate binding pockets S1/S2 that are close to the catalytic residues. The spacious substrate binding pockets S3/S4 contained residues are Asp164, Val165, Arg166, Glu167, Met208, Ala246, Pro247, Pro248, Tyr264, Gly266, Asn267, Tyr268, Gln269, Cys217, Gly271, Tyr273, Thr301 and Asp302 (39).

2.2. DAAs Optimization and Molecular Docking

The structures of the SARS-CoV-2 protease inhibitors were downloaded from the drug databank, DrugBank, (28). The geometry of all inhibitors was optimized using MMFF94 force field function of Avogadro software (34). Molecular Docking was applied using AutoDock Vina software (40), AutoDock Vina achieves approximately two orders of the magnitude speed-up

compared to AutoDock 4, in addition, it significantly improves the accuracy of the binding mode predictions.. The docking was rigid against the whole protein to examine the free natural affinity of binding ligand to substrate binding pockets and catalytic residues without forcing the docking of ligand to active site only. The docking was repeated 10 times for each ligand. The evaluation of affinity of docking depends on the docking scores and the probability to bind to the substrate binding pockets and the catalytic residues of the protein.

2.3. Analysis of Interactions between DAAs and SARS-CoV-2 PLpro

Nearly 61 direct-acting antiviral agents (DAA) have been reported to contemporary drugs in clinical trials for COVID-19 treatment where many of them were under molecular docking studies to identify the potent antiviral agents for COVID-19 (41), (42). Protein-Ligand Interaction Profiler (PLIP) web server (36) was used to analyze the interactions formed between DAAs and COVID-19 PLpro.

2.4. Molecular Dynamics Simulation and Molecular Docking

The molecular dynamics simulation of the PLpro was completed using the GROMACS all atom force field (37), (43). The protein was solvated, and the system was neutralized with the addition of Na^+ ions by replacing the water molecules. After completing those steps, the energy minimization of the system was then performed, which was followed by equilibration of the system using two consecutive runs, NVT (100 ps) and NPT (100 ps), respectively. Finally, the protein was introduced to 1000 ps molecular dynamics simulation with a time-stage of 2 fs for each simulation. The root mean square deviation (RMSD) of the peptide atom backbone and the radius of gyration (Rg) was plotted as a function of time (44). Compressed coordinates were measured every 10 ps (100 frames). Molecular Docking was finally performed for DAAs of the highest probability to bind to catalytic residues and different frames of PLpro MD.

2.5. SARS-CoV-2 PLpro Mutant C111S

SARS-CoV-2 PLpro mutant C111S solved structure was downloaded from the Protein Data Bank (PDB ID: 6WRH). The catalytic residues of PLpro mutant C111S are Ser111, His272 and Asp286. Molecular Docking was performed for DAAs of the highest probability to bind to catalytic residues and substrate binding-pocket of wild type COVID-19 PLpro (PDB ID: 6W9C) against the SARS-CoV-2 PLpro mutant C111S (PDB ID: 6WRH) to examine the efficacy of those DAAs against this mutant strain.

3. Results and Discussion

Molecular docking was performed on the solved structure (PDB ID: 6W9C) of SARS-CoV-2 PLpro. Table 1 lists the mean values of the docking scores and their probabilities to bind to catalytic residues and the substrate binding pockets S3/S4.

The results obtained shows Paritaprevir having the best docking score of -10.8 Kcal/mol, followed by Ledipasvir docking score of -10.38 Kcal/mol, and Elbasvir docking score of -9.94 Kcal/mol, however their probabilities to bind to the catalytic residues and substrate binding-pocket S3/S4 are found to be 0% for those ligands. Therefore, binding results are suggesting that those DAAs are not recommended to be used as potential treatment for SARS-CoV-2.

On the other hand, 4′-Tosyl Mycophenolic Acid-d3 of docking score -5.98 Kcal/mol has shown the highest probability of 50% to bind to the catalytic residues, followed by its parent Mycophenolic acid of docking score -5.72 Kcal/mol and probability of 30% to bind to catalytic residues and probability of 20% to S3/S4 pocket, then followed by Tamiflu of docking score -5.07 Kcal/mol with probability of 60% to bind to S3/S4 pocket, followed by Darunavir of docking score -6.7 Kcal/mol and probability of 60% to bind to S3/S4 pocket, then finally comes GRL 0617 of docking score -7.35 Kcal/mol and probability of 40% to bind to S3/S4 pocket. Therefore, those drugs have shown good docking scores with high native probabilities to bind to the active site pocket and are then suggested to be used as potential SARS-CoV-2 treatment with the preference to Mycophenolic Acid and 4′-Tosyl Mycophenolic Acid-d3. Figure. 1 shows the molecular docking between Mycophenolic Acid and 4′-Tosyl Mycophenolic Acid-d3 and SARS-CoV-2 PLpro protease, where SARS-CoV-2 PLpro is represented as cartoon and the catalytic residues PLpro Cys111, His272 and Asp286 are represented in blue color and their ligands are represented as licorice.

Table 1: Docking scores (Kcal/mol) calculated using AutoDock Vina against SARS-CoV-2 PLpro. The docking was repeated 10 times for each ligand and the probabilities to bind to catalytic residues and to active-site pocket (S3/S4) were calculated. The highest docking scores are highlighted in light green color and the highest probabilities are highlighted in orange color.

Drug Tested	ΔG (Kcal/mol)	Probability of binding to catalytic residues	Probability of binding to substrate binding-pocket (S3/S4)
Glecaprevir	-7.67 ± 0.21	0%	0%
Grazoprevir	-6.60 ± 0.09	0%	0%
Simeprevir	-7.62 ± 0.18	0%	0%
Voxilaprevir	-8.98 ± 0.04	0%	0%
Elbasvir	-9.94 ± 0.19	0%	0%
Beclabuvir	-7.72 ± 0.34	0%	0%
Ledipasvir	-10.38 ± 0.38	0%	0%
Remdesivir	-7.39 ± 0.2	0%	0%
Avigan	-6.40 ± 0.2	0%	10%
Tamiflu	-5.07 ± 0.2	0%	60%
Plaquenil	-5.16 ± 0.51	0%	10%
Paritaprevir	-10.80 ± 0.04	0%	0%
Daclatasvir	-9.52 ± 0.09	0%	0%

Mycophenolic acid	-5.72 ± 0.5	30%	20%
4'-Tosyl Mycophenolic Acid-d3	-5.98 ± 0.64	50%	0%
Ombitasvir	-9.72 ± 0.25	0%	0%
GRL 0617	-7.35 ± 0.41	0%	40%
GRL 0667	-7.55 ± 0.36	0%	0%
Lopinavir	-6.54 ± 0.57	0%	10%
Darunavir	-6.70 ± 0.61	0%	60%
Ritonavir	-5.80 ± 0.44	10%	0%

Protein-Ligand Interaction Profiler (PLIP) web server was used to analyze the interactions formed. Figure. 2 shows the formed interactions between the DAAs and SARS-CoV-2 PLpro protease after the docking, where ligands are shown in blue color, while the protein residues are shown in green color representations labeled with three-letter code. The H-bonds are shown in solid yellow lines, while the dashed red lines represent the hydrophobic interactions, and the green dashed lines represent the salt bridges and Pi-StackingP in dashed cyan lines. The results show two H-bonds formed between Mycophenolic Acid and His272 and Asp286 catalytic residues and one Pi-StackingP interaction with TRP 106, while 4′-Tosyl Mycophenolic Acid-d3 forms one H-bond with Gly163, two salt bridges with His272 catalytic residue, and one salt bridge with Lys174. The results obtained indicate that the formation of the hydrogen bonds and salt bridges with the active site pocket inhibits the function of the catalytic residues therefore prevent them from being shared in the virus replication.

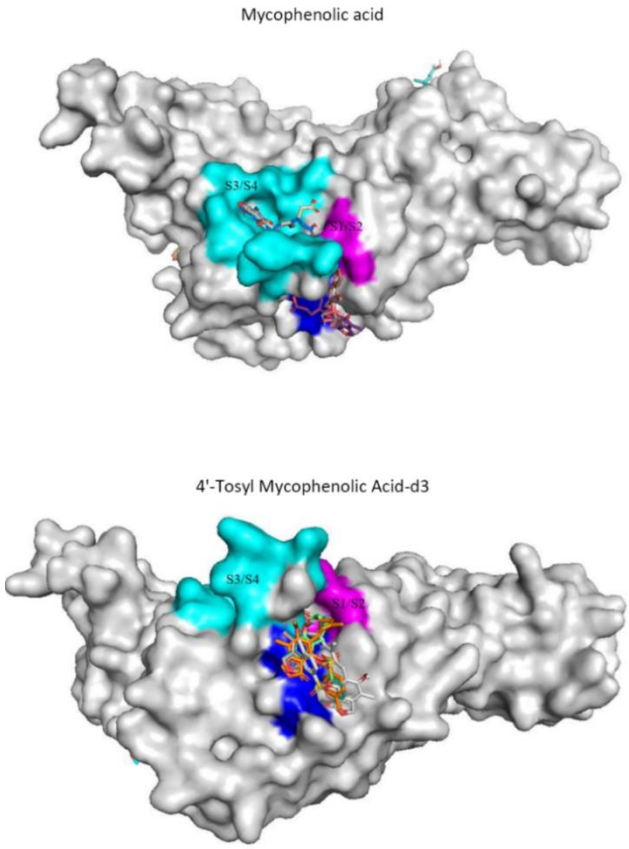

Figure. 1: Docking between Mycophenolic Acid and 4′-Tosyl Mycophenolic Acid-d3 and SARS-CoV-2 PLpro. SARS-CoV-2 PLpro is represented in gray color as surface, the catalytic (Cys111, His272 and Asp286) residues of PLpro are represented in blue color, substrate binding-pocket S1/S2 in magenta, substrate binding-pocket S3/S4 in cyan and ligands represented as licorice. 4′-Tosyl Mycophenolic Acid-d3 (-5.98 Kcal/mol) has the highest probability to bind to catalytic residues (50%) followed by its parent Mycophenolic acid (-5.72 Kcal/mol and 30% to bind to catalytic residues and 20% to substrate binding-pocket S3/S4).

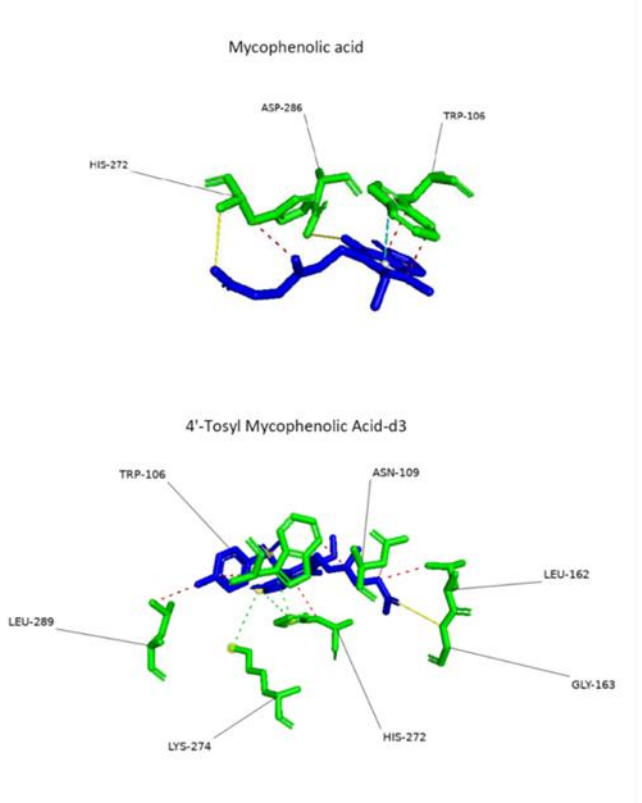

Figure. 2: Interactions formed after molecular docking using PLIP web server. Mycophenolic Acid and 4′-Tosyl Mycophenolic Acid-d3, represented in blue color, docked to SARS-CoV-2 PLpro (PDB ID: 6W9C), represented in green. H-bonds are shown in solid yellow lines while hydrophobic interactions are shown in red dashed lines. Salt bridges are represented in green dashed lines and Pi-StackingP are shown in dashed cyan. The results show two H-bonds formed between Mycophenolic Acid and the catalytic residues His272 and Asp286 and one Pi-StackingP interaction with TRP 106. The 4′-Tosyl Mycophenolic Acid-d3 forms one H-bond with Gly163, two salt bridges with catalytic residue His272 and one salt bridge with Lys174.

Interactions between the inhibitor and the protein are instantaneous through the molecular docking process making the interaction unstable. Therefore, the molecular dynamics simulation is used to allow us to provide the information about the stability of the molecular interactions on the formed complexes.

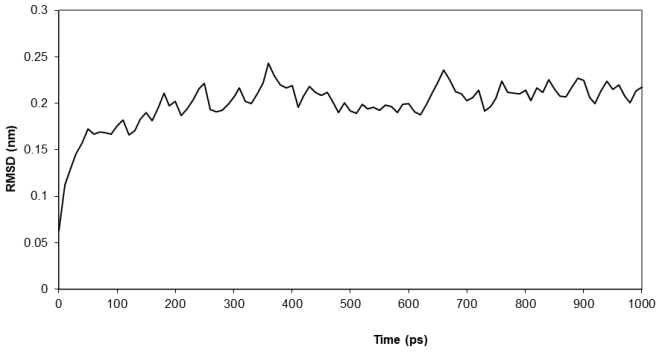

Figure. 3: Plot diagrams of Root Mean Square Deviation (RMSD) values for the backbone atoms of SARS-CoV-2 PLpro from the initial structure during 1000 ps simulation as a function of time.

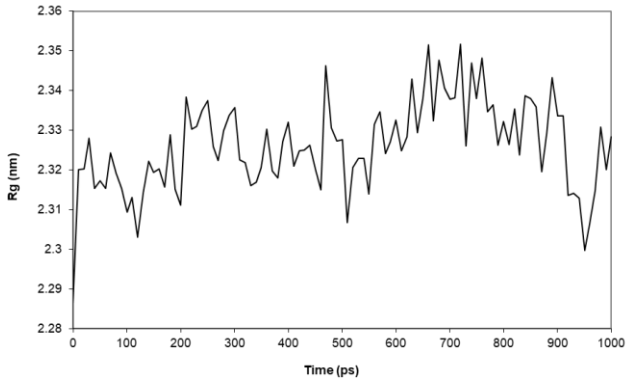

Figure. 4: Plot diagrams of radius of gyration (Rg) of SARS-CoV-2 PLpro through 1000 ps of molecular dynamics simulation.

Table 2: Docking scores (Kcal/mol) of Mycophenolic Acid and 4′-Tosyl Mycophenolic Acid-d3 against frames of MD of SARS-CoV-2 PLpro. The docking was repeated 10 times for each frame. The docking scores are stable over the different frames.

Frame	ΔG (Kcal/mol) Mycophenolic Acid	ΔG (Kcal/mol) 4′-Tosyl Mycophenolic Acid-d3
Frame 0 (0 ps)	-5.84 ± 0.35	-5.87 ± 0.36
Frame 10 (100 ps)	-6.23 ± 0.53	-5.13 ± 0.24
Frame 20 (200 ps)	-6.27 ± 0.49	-6.36 ± 0.43
Frame 30 (300 ps)	-5.95 ± 0.31	-6.74 ± 0.16
Frame 40 (400 ps)	-5.80 ± 0.54	-5.86 ± 0.24
Frame 50 (500 ps)	-5.69 ± 0.22	-6.14 ± 0.33
Frame 60 (600 ps)	-5.88 ± 0.36	-6.62 ± 0.24
Frame 70 (700 ps)	-6.17 ± 0.51	-6.10 ± 0.35
Frame 80 (800 ps)	-5.65 ± 0.37	-6.10 ± 0.33
Frame 90 (9000 ps)	-5.89 ± 0.24	-6.42 ± 0.47
Frame 100 (1000 ps)	-5.91 ± 0.35	-6.36 ± 0.24

In this research work, PLpro was used to perform molecular dynamics simulation. Figure. 3 shows the root mean square deviation (RMSD) values of PLpro dynamics simulation over 1000 ps, while the calculated radius of gyration (Rg) values over the simulation time scale are shown in Figure. 4. The RMSD and radius of gyration were chosen because they represent the stability of complex (i.e., the binding of inhibitor with protein over time). Molecular docking was then performed between Mycophenolic Acid and 4′-Tosyl Mycophenolic Acid-d3 and the different frames of PLpro MD are listed in Table 2 and the relation is represented in Figure. 5. The docking was repeated 10 times for every frame. The stability of the docking scores over the MD time indicates that Mycophenolic Acid and 4′-Tosyl Mycophenolic Acid-d3 form stable complexes with PLpro therefore indicating promise effectiveness for developing potential inhibitors for SARS-CoV-2.

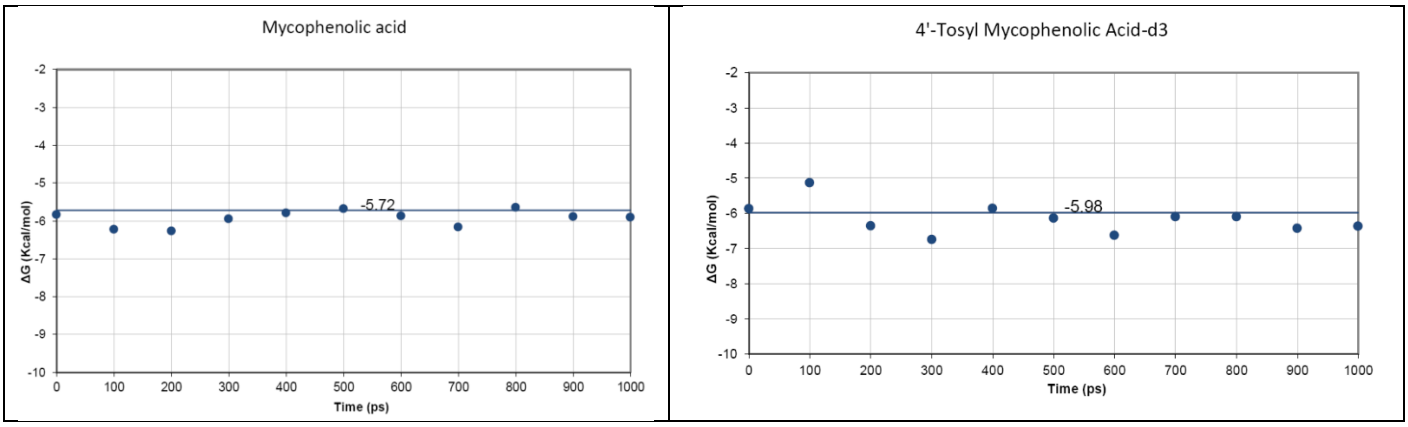

Figure. 5: The docking scores in Kcal/mol of Mycophenolic acid and 4′-Tosyl Mycophenolic Acid-d3 against the frames of MD of SARS-CoV-2 PLpro, shown in blue dots. The blue line is the docking score of PDB structure of PLpro. The docking was repeated 10 times for each frame, showing the docking scores are approximately stable over the different frames.

The alignment between the catalytic residues of the wild type of SARS-CoV-2 papain-like protease PLpro (PDB ID: 6W9C) and the PLpro mutant C111S protease (PDB ID: 6WRH) is displayed in Figure. 6. DAAs of the highest probabilities to bind to the catalytic residues and the substrate binding pocket S3/S4 of SARS-CoV-2 PLpro, including Mycophenolic acid, 4'-Tosyl Mycophenolic Acid-d3, Tamiflu, Darunavir and GRL 0617, were docked against SARS-CoV-2 PLpro mutant C111S protease to examine their efficacy against the mutant strain.

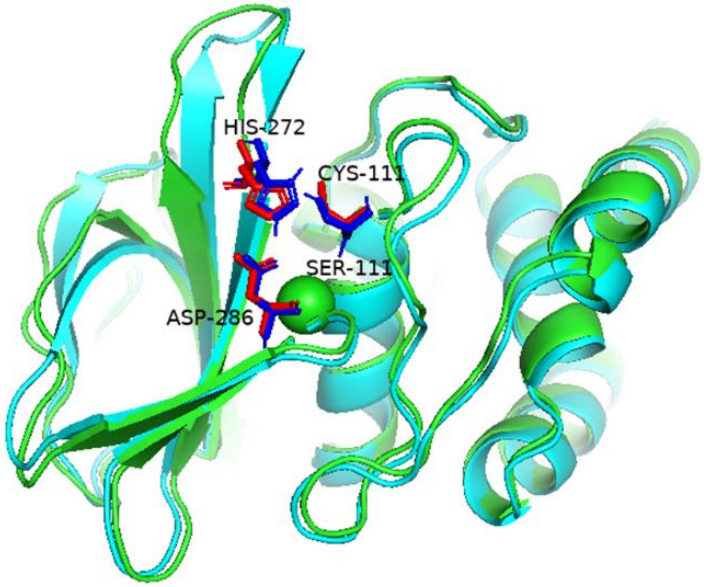

Figure. 6: The alignment between the active site of PLpro wild type SARS-CoV-2 (PDB ID: 6W9C), represented in green color, with catalytic residues, represented in red color, and SARS-CoV-2 PLpro mutant C111S (PDB ID: 6WRH) shown in cyan with the catalytic residues in blue.

Table 3: Docking scores (Kcal/mol) calculated by AutoDock Vina against SARS-CoV-2 PLpro mutant C111S (PDB ID: 6WRH). The docking was repeated 10 times for each ligand and the probabilities to bind to te catalytic residues and to the substrate binding-pocket (S3/S4) were calculated. The highest docking scores are heighted in light green and the highest probabilities are heighted in light orange color.

Drug Tested	ΔG (Kcal/mol)	Probability of binding to catalytic residues	Probability of binding to substrate binding-pocket (S3/S4)
Tamiflu	-5.50 ± 0.13	0%	0%
Mycophenolic acid	-5.47 ± 0.29	0%	20%
4'-Tosyl Mycophenolic Acid-d3	-6.31 ± 0.19	0%	10%
GRL 0617	-6.89 ± 0.39	0%	10%
Darunavir	-6.80 ± 0.43	0%	0%

Table 3 lists the mean values of the docking scores and the probabilities to bind to the catalytic residues and the substrate binding pocket S3/S4. The results obtained is showing Mycophenolic acid has the highest probability of 20% to bind to substrate binding pocket S3/S4 pocket, the results are demonstrated in Figure. 7, where all DAAs have no chance to bind to the catalytic residues, indicating that Mycophenolic acid could be of potential trial for therapeutics development for SARS-CoV-2 because the PLpro mutant C111S strain showed lower efficacy compared to the wild type of SARS-CoV-2 papain-like protease.

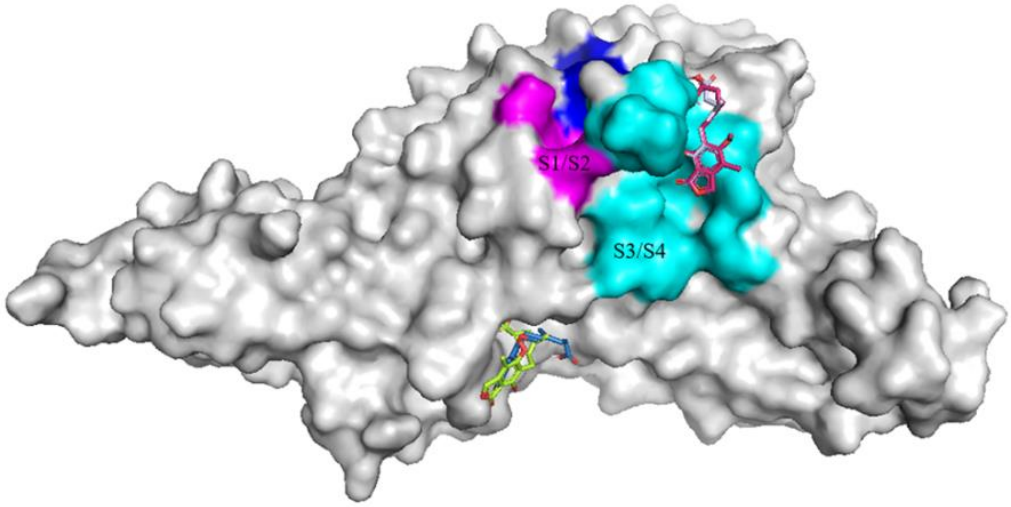

Figure. 7: Docking between Mycophenolic Acid and SARS-CoV-2 PLpro protease. SARS-CoV-2 PLpro mutant C111S represented in gray color as surface, catalytic (Ser111, His272 and Asp286) residues PLpro represented in blue color, substrate binding pocket S1/S2 in magenta, substrate binding pocket S3/S4 in cyan and the ligands represented as licorice. Mycophenolic acid (-5.47 Kcal/mol) shows the highest probability of 20% to bind to the substrate binding-pocket S3/S4.

4. Conclusion

The novel coronavirus SARS-CoV-2 is the reason behind the current worldwide pandemic of the respiratory coronavirus disease known as COVID-19. SARS-CoV-2 is considered one of the major pathogens that primarily targets the human respiratory system causing COVID-19 pneumonia. COVID-19 have shown less severe symptoms and a lower fatality rate compared to other SARS-CoV outbreaks; however, its transmission rate is faster compared to the other related SARS-CoV infections. The current study examined few different inhibitors currently used in the drug market, trying to repurpose those safe antiviral drugs as potential inhibitor against SARS-CoV-2. Our study results showed that Mycophenolic Acid and 4′-Tosyl Mycophenolic Acid-d3 molecular docking have the highest probability to bind to substrate binding pocket S3/S4 suggesting those drugs safe use as potent inhibitors against SARS-CoV-2.

The findings from this work gave us the insight to examine commonly used antiviral drugs against RNA dependent RNA polymerase to determine their inhibitors activity and to design an in-silico peptide inhibitor to inactivate the spike protein of SARS-CoV-2 virus.

References

1. Worldometer. COVID-19 CORONAVIRUS PANDEMIC [Internet]. Worldometer Data. 2020. Available from: https://www.worldometers.info/coronavirus
2. World Health Organization (WHO). Statement on the second meeting of the International Health Regulations (2005) Emergency Committee regarding the outbreak of novel coronavirus (2019-nCoV). [Internet]. Geneva: 30 Jan 2020. 2020. Available from: https://www.who.int/news-room/detail/30-01-2020-statement-on-the-second-meeting-of-the-international-health-regulations-(2005)-emergency-committee-regarding-the-outbreak-of-novel-coronavirus-(2019-ncov)
3. World Health Organization (WHO). WHO Director-General's opening remarks at the media briefing on COVID-19 - 11 March 2020. [Internet]. Geneva: 11 Mar 2020. 2020. Available from: https://www.who.int/dg/speeches/detail/who-director-general-s-opening-remarks-at-the-media-briefing-on-covid-19---11-march-2020
4. Cascella M, Rajnik M, Cuomo A, Dulebohn SC, Di Napoli R. Features, Evaluation and Treatment Coronavirus (COVID-19). StatPearls. 2020;
5. Hui DS, I Azhar E, Madani TA, Ntoumi F, Kock R, Dar O, et al. The continuing 2019-nCoV epidemic threat of novel coronaviruses to global health — The latest 2019 novel coronavirus outbreak in Wuhan, China. Int J Infect Dis. 2020;91:264–6.
6. Bogoch II, Watts A, Thomas-Bachli A, Huber C, Kraemer MUG, Khan K. Pneumonia of Unknown Etiology in Wuhan, China: Potential for International Spread Via Commercial Air Travel. J Travel Med. 2020;1–3.
7. Lu R, Zhao X, Li J, Niu P, Yang B, Wu H, et al. Genomic characterisation and epidemiology of 2019 novel coronavirus: implications for virus origins and receptor binding. Lancet. 2020;395(10224):565–74.
8. Wang W, Tang J, Wei F. Updated understanding of the outbreak of 2019 novel coronavirus (2019-nCoV) in Wuhan, China. J Med Virol. 2020;92(4):441–7.
9. Chan JFW, Lau SKP, To KKW, Cheng VCC, Woo PCY, Yue KY. Middle East Respiratory syndrome coronavirus: Another zoonotic betacoronavirus causing SARS-like disease. Clin Microbiol Rev. 2015;28(2):465–522.
10. Huang C, Wang Y, Li X, Ren L, Zhao J, Hu Y, et al. Clinical features of patients infected with 2019 novel coronavirus in Wuhan, China. Lancet. 2020;395(10223):497–506.
11. Ren L-L, Wang Y-M, Wu Z-Q, Xiang Z-C, Guo L, Xu T, et al. Identification of a novel coronavirus causing severe pneumonia in human. Chin Med J (Engl). 2020;1.
12. Elfiky AA, Ismail AM. Molecular modeling and docking revealed superiority of IDX-184 as HCV polymerase inhibitor. Future Virol. 2017;12(7):339–47.
13. Li Q, Guan X, Wu P, Wang X, Zhou L, Tong Y, et al. Early Transmission Dynamics in Wuhan,

China, of Novel Coronavirus–Infected Pneumonia. N Engl J Med. 2020;1199–207.
14. Hilgenfeld R. From SARS to MERS: crystallographic studies on coronaviral proteases enable antiviral drug design. FEBS J. 2014;281(18):4085–96.
15. Lim SP, Koh JHK, Seh CC, Liew CW, Davidson AD, Chua LS, et al. A crystal structure of the dengue virus non-structural protein 5 (NS5) polymerase delineates interdomain amino acid residues that enhance its thermostability and de novo initiation activities. J Biol Chem. 2013;288(43):31105–14.
16. Harcourt BH, Jukneliene D, Kanjanahaluethai A, Bechill J, Severson KM, Smith CM, et al. Identification of Severe Acute Respiratory Syndrome Coronavirus Replicase Products and Characterization of Papain-Like Protease Activity. 2004;78(24):13600–12.
17. Klemm T, Ebert G, Calleja DJ, Allison CC, Richardson LW, Bernardini JP, et al. Mechanism and inhibition of the papain-like protease , PLpro , of SARS-CoV- 2. 2020;1–17.
18. Békés M, Heden van Noort GJ van der, Ekkebus R, Ovaa H, Huang TT, Lima CD. Recognition of Lys48-Linked Di-ubiquitin and Deubiquitinating Activities of the SARS Coronavirus Papain-like Protease. Mol Cell [Internet]. 2016;19;62(4):572–85. Available from: doi: 10.1016/j.molcel.2016.04.016. PMID: 27203180; PMCID: PMC4875570
19. Barretto N, Jukneliene D, Ratia K, Chen Z, Mesecar AD, Baker SC. The Papain-Like Protease from the Severe Acute Respiratory Syndrome Coronavirus Is a Deubiquitinating Enzyme. J Virol [Internet]. 2005;79(24):15189–15198. Available from: doi: 10.1128/JVI.79.24.15189-15198.2005
20. Báez-Santos M. Y, John SE St., Mesecar AD. The SARS-coronavirus papain-like protease Structure, function and inhibition by designed antiviral compounds 1.pdf. Antiviral Res [Internet]. 2015;115:21–38. Available from: https://doi.org/10.1016/j.antiviral.2014.12.015
21. Snijder EJ, Bredenbeek PJ, Dobbe JC, Thiel V, Ziebuhr J, Poon LLM, et al. Unique and conserved features of genome and proteome of SARS-coronavirus, an early split-off from the coronavirus group 2 lineage. J Mol Biol. 2003;331(5):991–1004.
22. Thiel V, Ivanov KA, Putics Á, Hertzig T, Schelle B, Bayer S, et al. Mechanisms and enzymes involved in SARS coronavirus genome expression. J Gen Virol. 2003;84(9):2305–15.
23. Imbert I, Snijder EJ, Dimitrova M, Guillemot JC, Lécine P, Canard B. The SARS-Coronavirus PLnc domain of nsp3 as a replication/transcription scaffolding protein. Virus Res. 2008;133(2):136–48.
24. Angelini MM, Akhlaghpour M, Neuman BW, Buchmeier MJ. Severe acute respiratory syndrome coronavirus nonstructural proteins 3, 4, and 6 induce double-membrane vesicles. MBio. 2013;4(4):1–10.
25. Shin D, Mukherjee R, Grewe D, Bojkova D, Baek K, Geurink PP, et al. Papain-like protease regulates SARS-CoV-2 viral spread and innate immunity. Nature [Internet]. 2020;587(November). Available from: http://dx.doi.org/10.1038/s41586-020-2601-5
26. Serrano P, Johnson MA, Almeida MS, Horst R, Herrmann T, Joseph JS, et al. Nuclear Magnetic Resonance Structure of the N-Terminal Domain of Nonstructural Protein 3 from the Severe Acute Respiratory Syndrome Coronavirus. J Virol. 2007;81(21):12049–60.
27. Faesen AC, Luna-vargas MPA, Sixma TK. The role of UBL domains in ubiquitin-specific proteases. Biochem Soc Trans [Internet]. 2012;40:539–45. Available from: doi:%0A10.1042/bst20120004

28. Wishart DS, Feunang YD, Guo AC, Lo EJ, Marcu A, Grant R, et al. DrugBank 5.0 : a major update to the DrugBank database for 2018. Nucleic Acids Res [Internet]. 2018;46(November 2017):1074–82. Available from: https://doi.org/10.1093/nar/%0Agkx1037
29. Maiti BK. Can Papain-like Protease Inhibitors Halt SARS-CoV-2 Replication? ACS Pharmacol Transl Sci. 2020 Oct;3(5):1017–9.
30. Alamri MA, Tahir ul Qamar M, Mirza MU, Alqahtani SM, Froeyen M, Chen LL. Discovery of human coronaviruses pan-papain-like protease inhibitors using computational approaches. J Pharm Anal [Internet]. 2020;10(6):546–59. Available from: https://doi.org/10.1016/j.jpha.2020.08.012
31. Alfaro M, Alfaro I, Angel C. Identification of potential inhibitors of SARS-CoV-2 papain-like protease from tropane alkaloids from Schizanthus porrigens: A molecular docking study. Chem Phys Lett. 2020 Dec;761:138068.
32. Li D, Luan J, Zhang L. Molecular docking of potential SARS-CoV-2 papain-like protease inhibitors. Biochem Biophys Res Commun [Internet]. 2020/11/28. 2021 Jan 29;538:72–9. Available from: https://pubmed.ncbi.nlm.nih.gov/33276953
33. Kouznetsova VL, Zhang A, Tatineni M, Miller MA, Tsigelny IF. Potential COVID-19 papain-like protease PL(pro) inhibitors: repurposing FDA-approved drugs. PeerJ [Internet]. 2020 Sep 18;8:e9965–e9965. Available from: https://pubmed.ncbi.nlm.nih.gov/32999768
34. Hanwell MD, Curtis DE, Lonie DC, Vandermeersch T, Zurek E, Hutchison GR. Avogadro: an advanced semantic chemical editor, visualization, and analysis platform. J Cheminform [Internet]. 2012;4(1):17. Available from: https://doi.org/10.1186/1758-2946-4-17
35. Trott O, Olson AJ. AutoDock Vina: improving the speed and accuracy of docking with a new scoring function, efficient optimization, and multithreading. J Comput Chem [Internet]. 2010 Jan 30;31(2):455–61. Available from: https://pubmed.ncbi.nlm.nih.gov/19499576
36. Salentin S, Schreiber S, Haupt VJ, Adasme MF, Schroeder M. PLIP: Fully automated protein-ligand interaction profiler. Nucleic Acids Res. 2015;43(W1):W443–7.
37. Pronk S, Páll S, Schulz R, Larsson P, Bjelkmar P, Apostolov R, et al. GROMACS 4.5: A high-throughput and highly parallel open source molecular simulation toolkit. Bioinformatics. 2013;29(7):845–54.
38. Arya R, Das A, Prashar V, Kumar M. Potential inhibitors against papain-like protease of novel coronavirus (SARS-CoV-2) from FDA approved drugs. ChemRxiv. 2020;
39. Wishart DS, Wang WW, Tang J, Wei F, Salentin S, Schreiber S, et al. Pneumonia of Unknown Etiology in Wuhan, China: Potential for International Spread Via Commercial Air Travel. Nucleic Acids Res. 2020;395(2):441–7.
40. Anil KTJW. Autodock vina: improving the speed and accuracy of docking. J Comput Chem. 2019;31(2):455–61.
41. Morris DJ. Review Clinical trials of antiviral agents. 1992;97–103.
42. Adasme-Carreño F, Muñoz-Gutierrez C, Caballero J, Alzate-Morales H. J. Performance of the MM/GBSA scoring using a binding site hydrogen bond network-based frame selection: The protein kinase case. Phys Chem Chem Phys. 2014;16(27):14047–58.
43. Reva BA, Finkelstein A V., Skolnick J. What is the probability of a chance prediction of a protein

structure with an rmsd of 6 Å? Fold Des. 1998;3(2):141–7.
44. Gao Y, Yan L, Huang Y, Liu F, Zhao Y, Cao L, et al. Structure of the RNA-dependent RNA polymerase from COVID-19 virus. Science (80-). 2020;368(6492):779–82.